Pectin methylesterase activity is required for RALF1 peptide signalling output

Ann-Kathrin Rößling[1], Kai Dünser[1,2], Lothar Kalmbach[1], Elke Barbez[1], Jürgen Kleine-Vehn[1,2,3,#]

[1]Institute of Biology II, Division of Molecular Plant Physiology (MoPP), University of Freiburg, 79104 Freiburg, Germany
[2]Institute of Molecular Plant Biology (IMPB), Department of Applied Genetics and Cell Biology, University of Natural Resources and Life Sciences (BOKU), Vienna, 1190 Vienna, Austria
[3]Center for Integrative Biological Signalling Studies (CIBSS), University of Freiburg, 79104 Freiburg, Germany

[#]Correspondence should be addressed to juergen.kleine-vehn@biologie.uni-freiburg.de

Abstract:

The extracellular matrix plays an integrative role in cellular responses in plants, but its contribution to the signalling of extracellular peptides largely remains unknown. RAPID ALKALINIZATION FACTOR (RALF) are extracellular peptide hormones that play pivotal roles in various physiological processes. Here, we unveil a crucial connection between the demethylation machinery of the cell wall component pectin and RALF1 activity. Pectin is a polysaccharide homogalacturonan, contributing to the structural integrity of the cell wall. Our data illustrate that the pharmacological and genetic interference with PECTIN METHYL ESTERASEs (PMEs) abolishes RALF1 perception. Similarly, the application of free demethylated oligogalacturonides in the medium also reduces RALF1 activity. Accordingly, we conclude that RALF1 requires demethylated pectin to signal at the cell surface. We propose that demethylated and hence negatively charged pectin acts as a signalling scaffold for the positively charged RALF peptides, defining its output signalling. This mode of RALF peptide hormone signalling could shed light on a broader plant developmental context, linking extracellular matrix dynamics to hormone-mediated responses.

Introduction:

Plants perceive various external signals, but extracellular signal conceptualisation is poorly understood. Pectin is a polysaccharide homogalacturonan, contributing to the mechanical strength and integrity of the cell wall and plays a vital role in cell adhesion, growth, and signalling (Wolf, 2022). In the cell wall, PECTIN METHYL ESTERASEs (PMEs) catalyse the removal of methyl groups from the initially esterified pectin, giving rise to negatively charged carboxylic acid groups and altering the interaction of pectin with various extracellular components (Peaucelle et al., 2008). Here we address how pectin in the extracellular matrix contributes to the integration of RAPID ALKALINIZATION FACTORs (RALFs), which are cysteine-rich plant peptide hormones. RALF peptides are involved in multiple physiological and developmental processes, ranging from organ growth, pollen tube guidance to modulation of immune responses (Stegmann et al., 2017; Abarca et al., 2021). Catharanthus roseus receptor-like kinase 1-like (CrRLK1L) are transmembrane proteins with an extracellular domain, consisting of two adjacent malectin-like domains, for RALF signal perception and a cytoplasmic kinase domain for intracellular signal transduction (Escobar-Restrepo et al, 2007). FERONIA (FER) is currently the best characterized CrRLK1L, contributing to the above-mentioned developmental programs as well as the integration of environmental cues (Feng et al., 2018; Gigli-Bisceglia et al., 2022). On a cellular level, RALF binding to FER leads to rapid apoplastic (extracellular) alkalinisation (Haruta et al., 2014), which modulates cell wall properties, ion fluxes, and enzymatic activities, thereby influencing cellular expansion rates (Haruta et al., 2014; Barbez et al., 2017; Dünser et al., 2019). Besides its role in apoplastic pH, CrRLK1Ls play a role in cell wall sensing (Hematy et al., 2007; Höfte, 2015; Shih et al., 2014). The FER-dependent cell wall sensing mechanism involves the direct interaction with the extracellular LEUCINE-RICH REPEAT EXTENSINs (LRXs) (Dünser et al., 2019), suggesting that LRXs provide a physical link between FER and the cell wall (Herger et al., 2019). Despite its apparent importance, the integration of physical cell wall properties into surface signalling is mechanistically poorly understood. Here we report on the contribution of cell wall modification, such as the pectin demethylation, for RALF peptide hormone signalling.

Results and discussion:

Demethylated pectin may provide conceptualising information to the cell wall, but their contribution to RALF peptide activity has not been experimentally addressed. In order to interfere with the demethylation status of pectin, we initially used epigallocatechin gallate (EGCG), which is a natural inhibitor of PME (Lewis et al., 2008). The application of RALF1

peptides induces strong repression of main root growth in *Arabidopsis thaliana* (Haruta et al., 2014; Figure 1A). The application of EGCG also reduces main root growth but its co-treatment markedly interfered with the RALF1-induced reduction in root growth (Figure 1A, B). This raises the question of whether interference with PME blocks RALF-dependent regulation of root growth. To test the specificity of this EGCG effect on RALF1, we subsequently used flagellin22 (flg22), which is another root growth-repressing peptide. The flg22 peptide is derived from the N-terminus of bacterial flagellin and is known to elicit root growth repression via the innate immune receptor FLAGELLIN SENSITIVE2 (FLS2) (Chinchilla et al., 2006). EGCG treatments were not able to suppress, but further enhanced the FLG22-induced root growth repression (Figure 1C, D), suggesting a rather specific effect of EGCG on balancing RALF1 activity.

The structurally similar epicatechin (EC) is not an inhibitor of PMEs (Lewis et al., 2008) and was also not able to block RALF-induced root growth repression (Figure 1E, F), suggesting that the EGCG-induced interference with PME activity affects RALF1 responses. To consolidate this assumption, we employed the constitutive expression of *PECTIN METHYLESTERASE INHIBITOR 3* (*PMEI3*), which interferes with PME activity in the cell wall (Xu et al., 2022). *PMEI3* gain-of-function strongly reduced the RALF1-induced root growth repression (Figure 1G, H), being reminiscent of EGCG application.

We accordingly conclude that pharmacological and genetic interference with PME activity depresses the RALF1-sensitive root growth.

Next, we aimed to understand why PME activity is required for RALF1-dependent root growth control. FER-dependent perception of RALF peptides affects cell wall integrity. It is hence conceivable that the pharmacological and genetic interference with extracellular PME activity could counterbalance some extracellular effects of RALF1. The RALF1 effect on cell wall integrity was apparent in propidium iodide (PI)-stained cell walls of wild-type seedlings, showing swelling of the apoplastic signal and ectopic accumulations (Figure 2A, C). These RALF1-induced alterations were absent in PI-stained *fer-4* loss-of-function mutants (Figure 2B, C), suggesting that FER activation is required for this cellular effect. The pharmacological (Figure 2D, E) as well as genetic (Figure 2F-H) interference with PME activity phenocopied *fer-4* mutant phenotype and fully blocked the RALF1-induced alterations in cell wall labelling (Figure 2D-H). We hence conclude that interference with PME activity counterbalances RALF1-induced changes in the cell wall.

Next, we assessed whether PME activity defines RALF1 signalling output. To do so we addressed the RALF1 impact on apoplastic pH regulation, which is a primary readout of

RALF1 perception by FER (Haruta et al., 2014). We used 8-hydroxypyrene-1,3,6-trisulfonic acid trisodium salt (HPTS) as a fluorescent pH indicator for assessing apoplastic pH in epidermal root cells (Barbez et al., 2017). As expected, the application of RALF1 peptides induced an extracellular pH alkalization in wild-type epidermal root cells (Barbez et al., 2017; Figure 3A, B). In contrast, EGCG application as well as the overexpression of PMEI3, significantly reduced the RALF-induced alkalization of the apoplastic pH (Figure 3A-E). We accordingly conclude that interference with PME activity disrupts the primary output signalling of RALF.

Our data suggests that PME inhibition interferes with RALF signalling output, such as the alkalinisation of the cell wall, ultimately affecting cell wall properties and root growth. To assess if PME activity affects the extracellular perception of RALF1, we looked into ligand induced cellular dynamics of its receptor FER. An early event of receptor-mediated signalling often involves the ligand-induced endocytosis of the receptor as has been previously demonstrated for the RALF1-receptor FER (Yu et al., 2020). Therefore, we next tested whether the RALF ligand-induced endocytosis of FER is altered upon changes in the methylation status of the cell wall. In agreement with previous reports, we observed RALF1-dependent internalization of functional pFER::FER-GFP in epidermal root cells (Figure 3F, G). On the other hand, the ligand-induced internalization of FER-GFP was abolished when we pharmacologically or genetically suppressed PME activity (Figure 3F-J). These findings propose that the PME activity is required for the earliest events of RALF1 perception by FER.

LRX proteins bind to RALF peptides (Moussu et al., 2020) and link FER signalling with a cell wall sensing mechanism (Dünser et al., 2019). Therefore, we tested if the PME-dependent control of RALF1-reliant root growth requires LRX proteins. The EGCG-induced repression of RALF was not altered in the *lrx1 lrx2 lrx3 lrx4 lrx5* quintuple mutants when compared to wild-type roots (Figure 4A-D). This finding indicates that the LRX protein family is not required to define the PME-dependent signalling output of RALF peptides.

Considering that the pectin demethylation machinery defines RALF signalling independently of the LRX-dependent cell wall sensing mechanism, we assumed a rather direct integration of the demethylation status of pectin and RALF peptide signalling. Demethylated pectin is negatively charged. Notably, RALF1 contains in total 8 positively charged amino acids (3 lysine (K) and 5 arginine (R)), providing the positive net charges to the RALF1 peptide at the pH of the cell wall (Figure 5A, B). These residues could potentially enable demethylated pectin binding, which would be in analogy to the well-characterised demethylated pectin binding protein POLYGALACTURONASE-INHIBITING PROTEIN (PGIP). PGIP binds to

demethylated pectin through a positively charged binding site, which is formed by clustered residues of lysine (K) and arginine (R) (Spadoni et al., 2006). To initially test if the positive charges in RALF1 are essential for its bioactivity, we synthesized a RALF1-like peptide by substituting the K and R residues (*RALF1*$^{-KR}$), creating a slightly negatively charged peptide in the pH range of the cell wall (Figure 5A, C). *RALF1*$^{-KR}$ peptides are not bioactive, because they did neither affect root growth, or cell wall integrity, nor did they induce the ligand-induced endocytosis of FER (Figure 5D-I). These findings suggest that the positively charged residues in RALF1 are essential for RALF activity.

It is conceivable that positively charged RALF1 peptides associate with the negatively charged demethylated pectin. To assess this, we added demethylated oligogalacturonides (OGs) into the growth medium and tested their impact on RALF1 perception. Notably, the addition of free, demethylated OGs into the media did not visibly affect the cell wall or FER endocytosis on its own (Figure 6A-D). On the other hand, when co-treated with RALF1 peptides, free OGs in the medium strongly interfered with RALF1-induced cell wall swelling and with RALF ligand-induced endocytosis of its FER receptor (Figure 6A-D). This suggests that demethylated OGs in the media restrain RALF1 peptides and thereby limit the RALF1 activity at the root surface.

Concluding remarks:

Here we illustrate that the PME activity is required for RALF1-dependent control of root growth. This inhibitory effect relates to the disruption of RALF signalling output. We accordingly propose that the generation of demethylated, charged pectin in the cell wall is required for RALF1 signalling at the root surface. LRX proteins directly interact with FER and thereby contribute to cell wall sensing (Dünser et al., 2019), but the LRX family is not required for the here proposed conceptualising effect on RALF signalling.

Demethylated pectin may directly associate with RALF1 peptides because demethylated OGs fragments in the medium are able to abolish the cellular effects of RALF1 peptide. The positive charges in RALF peptides are crucial for their bioactivity and it is tempting to speculate that positively charged RALF peptides interact with demethylated, and hence negatively charged pectin. This particular aspect certainly awaits further biochemical characterisation.

Based on our findings, we envision that negatively charged, demethylated pectin could function as a signalling scaffold for positively charged RALF peptides, which seems crucial for its signalling via the FER receptor. Recently it has been suggested that FER can bind to de-

methylated pectin (Feng et al., 2018; Lin et al., 2022; Gigli-Bisceglia et al., 2022). It is hence conceivable that de-methylated pectin directly contributes to RALF activity by affecting its molecular interaction with FER. A detailed biochemical and structural analysis of the binding of galacturonides and RALF peptides to the FER receptor, as well as the possibly simultaneous binding of both to FER, will further dissect this crucial step in the molecular interplay of RALF and FER signalling.

The here proposed mechanism could link the pectin-related cell wall status with peptide hormone signalling, providing a conceptualising extracellular signalling scaffold. This could also lead to self-emerging feedback properties because high extracellular PME activity is expected to strongly acidify the apoplast (Wolf et al., 2009), which in turn would be counteracted by the demethylated pectin-dependent activation of RALF peptides and its consequences on apoplast alkalinisation (Haruta et al., 2014; Barbez et al., 2017; this study).

Figure legends

Figure 1. PME activity is required for RALF1-induced root growth repression

(A-B) Three-day-old wild-type seedlings were subjected for three days to 1 µM RALF1 and/or 2.5 µM EGCG (A). (B) Boxplots depict the root length of wild-type seedlings under different treatments shown in (A).

(C-D) Three-day-old wild-type seedlings were exposed for three days with 0.5 µM flg22 and 15 µM EGCG or solvent control (C). (D) Boxplots depict the root length of wild-type seedlings under different treatments shown in (C).

(E-F) Three-day-old wild-type seedlings transferred for three days to solvent control, 1 µM RALF1 and/or 15 µM EC (E). (F) Boxplots depict root length of wild-type seedlings under different treatments shown in (E).

(G-H) Three-day-old wild-type and 35S::PMEI3 seedlings were exposed for three days to 1 µM RALF1 or solvent control (G). (H) Boxplots depict the root length of wild-type compared to 35S::PMEI3 seedlings of the treatments shown in (G).

Statistical significance was determined by a one-way ANOVA with a Tukey Post Hoc multiple comparisons test ($P < 0.05$, letters indicate significance categories) (B, D and F) or a two-way ANOVA with Bonferroni Post Hoc test (**** = $P < 0.0001$) (H). Boxplots: Box limits are representing the 25th and 75th percentile, the horizontal line represents the median. Whiskers

display min. to max. values. Representative experiments are shown. (Scale bar = 1 cm, n = 11 – 13 roots per treatment/line).

Figure 2. RALF1 requires PME activity to affect cell wall integrity

(A-C) Confocal microscopy images of the root epidermal cells of 6-day-old wild-type (A) and *fer-4* mutant (B) seedlings, treated for 3 h with 1 µM RALF1 or solvent control. Seedlings were mounted in propidium iodide to visualize the cell walls. Arrowheads indicate RALF1-induced alterations of the cell wall stain. (C) Graphs represent the width of PI signal per root under different treatments shown in (A,B). (n = 9 – 11 roots per treatment with a total number of 49 – 51 quantified cells).

(D-E) Confocal microscopy images (D) and quantification (E) of 6-day-old roots of wild-type seedlings, treated in liquid medium with 1 µM RALF1 or solvent control for 3 h. Seedlings were mounted in propidium iodide to visualize the cell walls. Arrowheads indicate cell wall invaginations. (n = 8 – 10 roots per treatment with a total number of 44 – 49 quantified cells).

(F-H) Confocal microscopy images (F, G) and quantification (H) of 6-day-old wild-type (F) and 35S::PMEI3 (G) roots, treated in liquid medium with 1 µM RALF1 or solvent control for 3 h. Seedlings were mounted in propidium iodide to visualize the cell walls. Arrowheads indicate cell wall invaginations. (n = 8 – 12 roots per treatment with a total number of 46 – 53 quantified cells).

Statistical significance was determined by a one-way ANOVA with a Tukey Post Hoc multiple comparisons test ($P < 0.05$, letters indicate significance categories) (E) or a two-way ANOVA with Bonferroni Post Hoc test (**** = $P < 0.0001$) (C and H). Boxplots: Box limits are representing the 25th and 75th percentile, the horizontal line represents the median. Whiskers display min. to max. values. (Scale bar = 25 µm).

Figure 3. PME activity is required for RALF1 signalling output

(A-B) HPTS-based (458/405 ratio) pH assessment of late meristematic root cells of wild-type seedlings treated for 3h with 1 µM RALF1, 50 µM ECGC or both compared to solvent control. Representative confocal images (A) are shown (scale bar = 10 µm). (B) Boxplots depict mean HPTS 458/405 intensities shown in (A), n = 9 – 11.

(C-D) HPTS-based (458/405 ratio) pH assessment of late meristematic cells in wild-type and 35S::PMEI3 seedlings treated for 3h with 1 µM RALF1 compared to solvent control. (scale bar = 10 µm). (D) Boxplots depict mean HPTS 458/405 intensities shown in (C), n = 10 – 12.

(F-G) RALF1-induced internalization of FER::FER-GFP in late meristematic epidermal root cells of seedlings treated for 3h with 1 µM RALF1, 50 µM ECGC or both compared to solvent control.–(scale bar = 25 µm). (G) Boxplots displaying the mean intracellular GFP signal intensity shown in (F), n = 9 – 12.

(H-J) RALF1-induced internalization of FER::FER-GFP in late meristematic epidermal root cells in wild-type (H) and in 35S::PMEI3 (I) seedlings treated for 3h with 1 µM RALF1 compared to solvent control. (J) Boxplots displaying the intracellular GFP signal intensity shown in (H and I).

Statistical significance was determined by a one-way ANOVA with a Tukey Post Hoc multiple comparisons test ($P < 0.05$, letters indicate significance categories) (B and G) or a two-way ANOVA with Bonferroni Post Hoc test (**** = $P < 0.0001$) (D and J). Boxplots: Box limits are representing 25th and 75th percentile, the horizontal line represents the median. Whiskers display min. to max. values.

Figure 4. LRX proteins are not essential for the PME-dependent activity of RALF1

(A-D) Three-day-old wild-type (A) or *lrx1/lrx2/lrx3/lrx4/lrx5* quintuple mutant (C) seedlings transferred for three days in liquid growth medium supplemented with solvent control, 1 µM RALF1 and/or 15 µM EGCG. Seedlings were transferred to solid growth medium just before imaging. (B, D) Boxplots display root length of seedlings under different treatments shown in (A,C).

Statistical significance was determined by a one-way ANOVA with a Tukey Post Hoc multiple comparisons test ($P < 0.05$, letters indicate significance categories) (B and D). (Scale bar = 1 cm, n = 14 – 16 roots per treatment/line). Boxplots: Box limits are representing 25th and 75th percentile, the horizontal line represents the median. Whiskers display min. to max. values. Representative experiments are shown.

Figure 5. Positive charges in RALF1 are required for its bioactivity

(A-C) Amino acid composition of RALF1 and non-charged RALF1^{-KR} peptides and its respective pH-dependent net charge (B, C).

(D, E) Three-day-old wild-type seedlings were exposed for three days to 1 µM RALF1 or RALF1^{-KR} or solvent control (D). (E) Boxplots display root length of seedlings under different treatments shown in (D). (Scale bar = 1 cm, n = 14 – 15).

(F, G) Confocal images of 6-day-old wild-type roots after 3 h treatment in liquid medium with 1 µM RALF1 or RALF1^{-KR} or solvent control. Seedlings were mounted in propidium iodide to

visualize the cell walls. Arrowheads indicate cell wall invaginations (F). (G) Graphs represent the average cell wall width per root under different treatments shown in (F). (Scale bar = 25 µm, n = 9 – 12).

(H, I) RALF1-induced internalization of FER::FER-GFP in late meristematic epidermal root cells of 6-day-old seedlings treated for 3h with solvent control, 1 µM RALF1 or RALF1^{-KR}. Representative confocal images (H) are shown (Scale bar = 25 µm). (I) Boxplots display the FER-GFP signal intensity. (n = 11 – 12 roots per treatment with a total number of 50 – 56 quantified cells).

Statistical significance was determined by a one-way ANOVA with a Tukey Post Hoc multiple comparisons test ($P < 0.05$, letters indicate significance categories) (E, G and I). Boxplots: Box limits are representing 25th and 75th percentile, the horizontal line represents the median. Whiskers display min. to max. values. Representative experiments are shown.

Figure 6. Application of free demethylated oligogalacturonides disrupts RALF1 activity at the cell surface

(A, B) Confocal images of 6-day-old wild-type roots after 3 h treatment in liquid medium with solvent control, OG$^{10-15}$, OG$^{25-50}$ and 1 µM RALF1, respectively (A). Seedlings were mounted in propidium iodide to visualize the cell walls. Arrowheads indicate cell wall invaginations. (B) Graphs represent the average cell wall width per root under different treatments shown in (A), (n = 8 – 11 roots per treatment with a total number of 46 – 52 quantified cells).

(C, D) RALF1-induced internalization of FER::FER-GFP in late meristematic epidermal root cells of 6-day-old seedlings treated for 3h with solvent control, OG$^{10-15}$, OG$^{25-50}$ and 1 µM RALF1, respectively. (D) Boxplots display the intracellular FER-GFP signal intensities. (n = 10 – 11).

Statistical significance was determined by a one-way ANOVA with a Tukey Post Hoc multiple comparisons test ($P < 0.05$, letters indicate significance categories) (B and D). Scale bar = 25 µm Boxplots: Box limits are representing 25th and 75th percentile, the horizontal line represents the median. Whiskers display min. to max. values. Representative experiments are shown.

Figure 7. Working model on pectin-dependent control of RALF activity

Demethylated and hence negatively charged pectin is crucial for the signalling output of positively charged RALF peptides. Either the interference with PME activity, application of free demethylated OGs, or removal of positive charges in RALF lead to abolished RALF output signalling.

Material and methods

Plant material and growth conditions

All experiments were carried out in *Arabidopsis thaliana*, ecotype *Col-0*. The following plant lines were described in previous publications: 35S::PMEI3 (Lionetti et al., 2017), *lrx1/lrx2/lrx3/lrx4/lrx5* (Dünser et al., 2019), FER::FER-GFP (in *fer-4*, Shih et al., 2014), *fer-4* (Shih et al., 2014), FER::FER-GFP x 35S::PMEI3 (in *fer-4*, obtained by crossing). After surface sterilization in 70% and 100% ethanol, seeds were vernalized at 4°C for 2 days in darkness, afterwards grown vertically on ½ strength Murashige and Skoog (MS) medium plates containing 1% sucrose in a long-day regime (16 h light and 8 h darkness) at 21 °C.

Chemicals and peptides

All chemicals were dissolved in dimethyl sulfoxide (DMSO) and served as solvent control, unless indicated otherwise. We used Propidium iodide (PI) in a working concentration of 0.02 mg/mL for cell wall counterstaining (obtained from Sigma (MO, USA)). Epigallocatechin gallate (EGCG) was used to interfere with PME activity in liquid treatments (obtained from Cayman Chemical (MI, USA)), epicatechin (EC) was used as negative control (from Cayman Chemical (MI, USA)) and flg22 peptides as a peptide control (obtained from Sigma (MO, USA)). The RALF1 peptide (mature RALF1, with the amino acid sequence: ATTKYISYQSLKRNSVPCSRRGASYYNCQNGAQANPYSRGCSKIARCRS) and the non-charged RALF1^{-KR} peptide version (amino acid sequence: ATTSYISYQSLTSNSVPCSDTGASYYNCQNGAQANPYSDGCSYIASCRS) were both synthesized by PSL GmbH (Heidelberg, Germany) and dissolved in water. The uncharged RALF1^{-KR} peptide was obtained by changing the 8 positively charged amino acids randomly into uncharged ones (either S, Y, D, E or T). The galacturonan oligosaccharides OG$^{10-15}$ and OG$^{25-50}$ were obtained from Elicityl (Crolles, France) and Biosynth (Staad, Switzerland), respectively.

Confocal microscopy

For image acquisition, an upright Leica TCS SP8 FALCON FLIM confocal laser scanning microscope, equipped with a Leica HC PL APO Corr 63 x 1.20 water immersion CS2 objective, was used. GFP was excited at 488 nm (fluorescence emission: 500 - 550 nm), PI at 561 nm (fluorescence emission: 640 - 750 nm). Experiments assessing apoplastic pH were carried out as previously described (Barbez et al., 2017) using 8-hydroyypyrene-1,3,6-trisulfonuc acid trisodium salt (HPTS; Sigma-Aldrich). In brief, roots of 6-day-old seedlings were treated for 3

h in liquid ½ MS medium containing 1 µM RALF1 and/or 50 µM EGCG or the appropriate amount of solvent control (water or DMSO, respectively) for 3 h. If not mentioned otherwise, pharmacological treatments have been performed in liquid medium in multiwell plates. Prior to imaging, the roots were mounted on a solid block of ½ MS medium containing 1 mM HPTS. The block was transferred to a microscopy slide and imaged with a coverslip on top. Image processing was performed as previously described (Barbez et al., 2017) using a macro for Fiji. Four transversal cell walls were quantified per root. The protonated form of HPTS was excited at 405 nm and 0.5% Diode UV laser intensity, and the deprotonated form at 455 nm with 30% Argon laser intensity. Images here were obtained in sequential scan mode. Z-stacks were recorded with a step size of 420 nm, with a stack containing 20 slices on average. The Gain of the HyD detectors (or PMT for HPTS experiments) stayed constant during imaging. The pinhole was set to 111.4 µm (for HPTS experiments to 196 µm). To counterstain the cell walls, roots were mounted in PI solution (0.02 mg/mL) prior to imaging. The signal intensity of intracellular space or plasma membrane was assessed using Fiji, with four cells analyzed per root. The ROI stayed constant over the experiments and biological replicates. For quantification of the PI staining width (and therefore the thickness of the cell wall) the thickness of transversal and longitudinal sections stained by PI were measured using Fiji, with four to six stained plasma membranes quantified per root. For the RALF1-treated roots, only the invaginated regions were chosen for analysis.

Root length analysis and root growth assay

For root growth assays, seedlings were grown for 3 days on solid ½ MS plates. Afterwards, they are transferred into 3 mL of liquid ½ MS medium containing RALF1 and/or EGCG or the appropriate amount of solvent control (water or DMSO, respectively). After 3 days of growth in liquid media with gentle agitation on a platform shaker, the seedlings were placed on solid ½ MS plates and scanned using a flat bed scanner. Root length was measured using Fiji. For statistical analyses, the GraphPad Prism Software (version 9.5.1) was used.

In silico analysis

For assessment of the charge of the RALF1 and RALF1-KR peptide, the Peptide Calculator Online tool from https://www.biosynth.com/peptide-calculator was used.

Acknowledgements

We are grateful to Gabriele Monshausen and Grégory Mouille for sharing published material; our team members for helpful discussions; and the LIC Imaging Center Freiburg for expertise and support. This work was supported by the Austrian Science Fund (FWF) (P33044 to J.K.-V.,), and the German Science fund (DFG; 470007283 to J.K.-V. and CIBSS – EXC-2189 Project ID 390939984 to J.K.-V. and to E.B.).

References

Abarca, D., Pizarro, L., Hernández-Blanco, C., Sánchez-Vallet, A., & Sánchez-Rodríguez, C. (2021). RALF peptides as master regulators of plant reproduction: Structural conservation amid functional divergence. The Plant Cell, 33(4), 1036-1041.

Barbez, E., Kubes, M., Rolčík, J., Béziat, C., Pěnčík, A., Wang, B., ... & Benková, E. (2017). A novel putative auxin carrier family regulates intracellular auxin homeostasis in plants. Nature, 485(7396), 119-122.

Chinchilla, D., Bauer, Z., Regenass, M., Boller, T., & Felix, G. (2006). The Arabidopsis receptor kinase FLS2 binds flg22 and determines the specificity of flagellin perception. The Plant Cell, 18(2), 465-476.

Dünser, K., Gupta, S., Herger, A., Feraru, M. I., Ringli, C., & Kleine-Vehn, J. (2019). Extracellular matrix sensing by FERONIA and LEUCINE-RICH REPEAT EXTENSIN proteins is required for cellulose synthesis. Plant Physiology, 180(4), 2230-2248.

Escobar-Restrepo, J. M., Huck, N., Kessler, S., Gagliardini, V., Gheyselinck, J., Yang, W. C., ... & Grossniklaus, U. (2007). The FERONIA receptor-like kinase mediates male–female interactions during pollen tube reception. Science, 317(5838), 656-660.

Feng, W., Kita, D., Peaucelle, A., Cartwright, H. N., Doan, V., Duan, Q., ... & Brady, S. M. (2018). The FERONIA receptor kinase maintains cell-wall integrity during salt stress through Ca2+ signaling. Current Biology, 28(5), 666-675.

Gigli-Bisceglia, N., Engelsdorf, T., Hamann, T., & Ranf, S. (2022). Cysteine-rich receptor-like kinases and their ligands: Key regulators of plant immunity. New Phytologist, 233(4), 1449-1463.

Haruta, M., Sabat, G., & Stecker, K. (2014). RACK1 has dual roles in abscisic acid signaling and in coordination of cell division and cell expansion in Arabidopsis thaliana. Plant & Cell Physiology, 55(12), 2090-2102.

Hematy, K., Sado, P. E., Van Tuinen, A., Rochange, S., Desnos, T., Balzergue, S., ... & Höfte, H. (2007). A receptor-like kinase mediates the response of Arabidopsis cells to the inhibition of cellulose synthesis. Current Biology, 17(11), 922-931.

Herger, A., Dünser, K., & Kleine-Vehn, J. (2019). Ring-like FERM proteins: Integrators of cell mechanics and growth dynamics. Journal of Experimental Botany, 70(2), 383-391.

Höfte, H. (2015). The yin and yang of cell wall integrity control: Brassinosteroid and FERONIA signaling. The Plant Cell, 27(12), 2946-2947.

Lewis, N. G., Davin, L. B., & Dinkova-Kostova, A. T. (2008). Recognition and manipulation of plant cell wall architecture by pathogenic microbes. Fungal Genetics and Biology, 45(4), 275-281.

Lin, Y., Ding, X., Cao, C., Chen, Z., Zhou, J., Li, Y., ... & Li, C. (2022). Structural insights into FERONIA-mediated RALF signaling. Genes & Development, 36(9-10), 796-802.

Moussu, S., Ladouce, N., de Billy, F., Vasseur, F., Vaissayre, V., Grison, M., ... & Ndiaye, S. (2020). A receptor-like kinase specifies symbiotic bacterial infection in Medicago truncatula. PLoS Genetics, 16(2), e1008632.

Peaucelle, A., Braybrook, S. A., Le Guillou, L., Bron, E., Kuhlemeier, C., & Höfte, H. (2008). Pectin-induced changes in cell wall mechanics underlie organ initiation in Arabidopsis. Current Biology, 18(12), 1845-1854.

Shih, H. W., Miller, N. D., Dai, C., Spalding, E. P., & Monshausen, G. B. (2014). The receptor-like kinase FERONIA is required for mechanical signal transduction in Arabidopsis seedlings. Current Biology, 24(16), 1887-1892.

Spadoni, S., Cervone, F., & De Lorenzo, G. (2006). Interaction between fungal polygalacturonases and their proteinaceous inhibitor: A computational study. Proteins: Structure, Function, and Bioinformatics, 64(1), 219-230.

Stegmann, M., Monaghan, J., Smakowska-Luzan, E., Rovenich, H., Lehner, A., Holton, N., ... & Zipfel, C. (2017). The receptor kinase FER is a RALF-regulated scaffold controlling plant immune signaling. Science, 355(6322), 287-289.

Wolf, S., & Hématy, K. (2012). Growth control and cell wall signaling in plants. Annual Review of Plant Biology, 63, 381-407.

Figure 1.

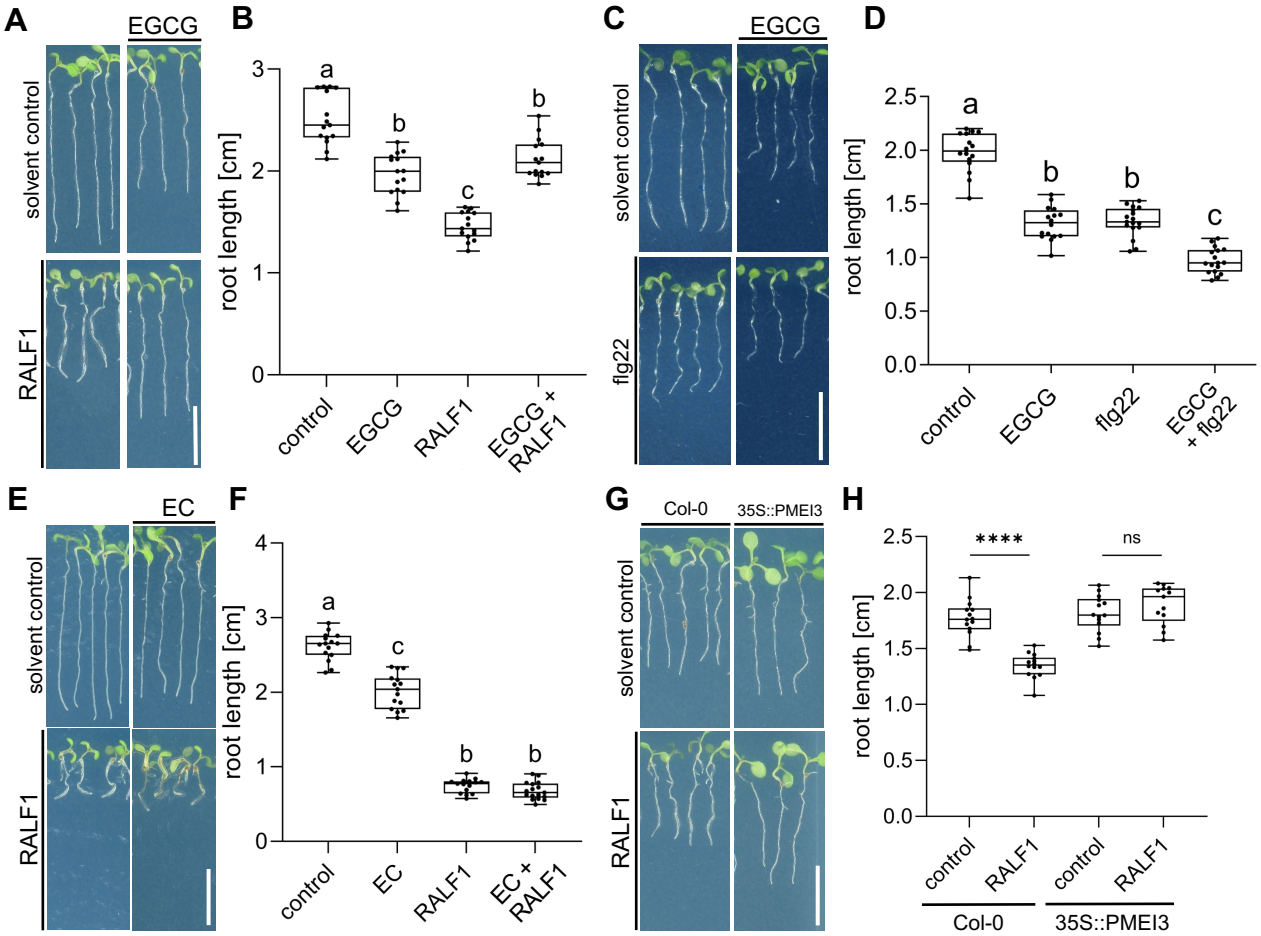
A
EGCG
solvent control
RALF1
B
root length [cm]
a
b
c
b
control
EGCG
RALF1
EGCG + RALF1
C
EGCG
solvent control
flg22
D
root length [cm]
a
b
b
c
control
EGCG
flg22
EGCG + flg22
E
EC
solvent control
RALF1
F
root length [cm]
a
c
b
b
control
EC
RALF1
EC + RALF1
G
Col-0
35S::PMEI3
solvent control
RALF1
H
root length [cm]
****
ns
control
RALF1
control
RALF1
Col-0
35S::PMEI3

Figure 2.

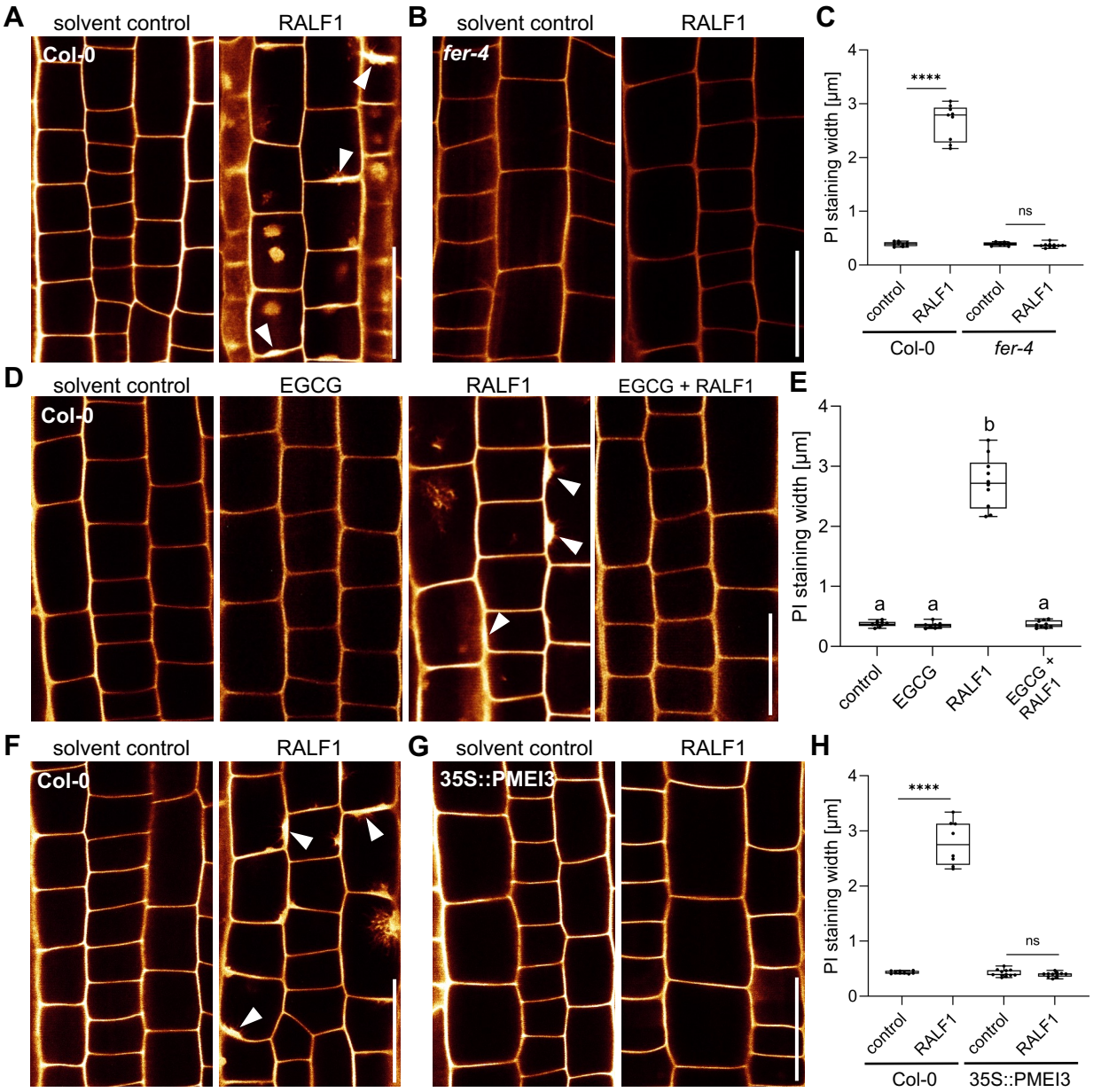
A
solvent control
RALF1
Col-0
B
solvent control
RALF1
fer-4
C
PI staining width [µm]
****
ns
control
RALF1
control
RALF1
Col-0
fer-4
D
solvent control
EGCG
RALF1
EGCG + RALF1
Col-0
E
PI staining width [µm]
a
a
b
a
control
EGCG
RALF1
EGCG + RALF1
F
solvent control
RALF1
Col-0
G
solvent control
RALF1
35S::PMEI3
H
PI staining width [µm]
****
ns
control
RALF1
control
RALF1
Col-0
35S::PMEI3

Figure 3.

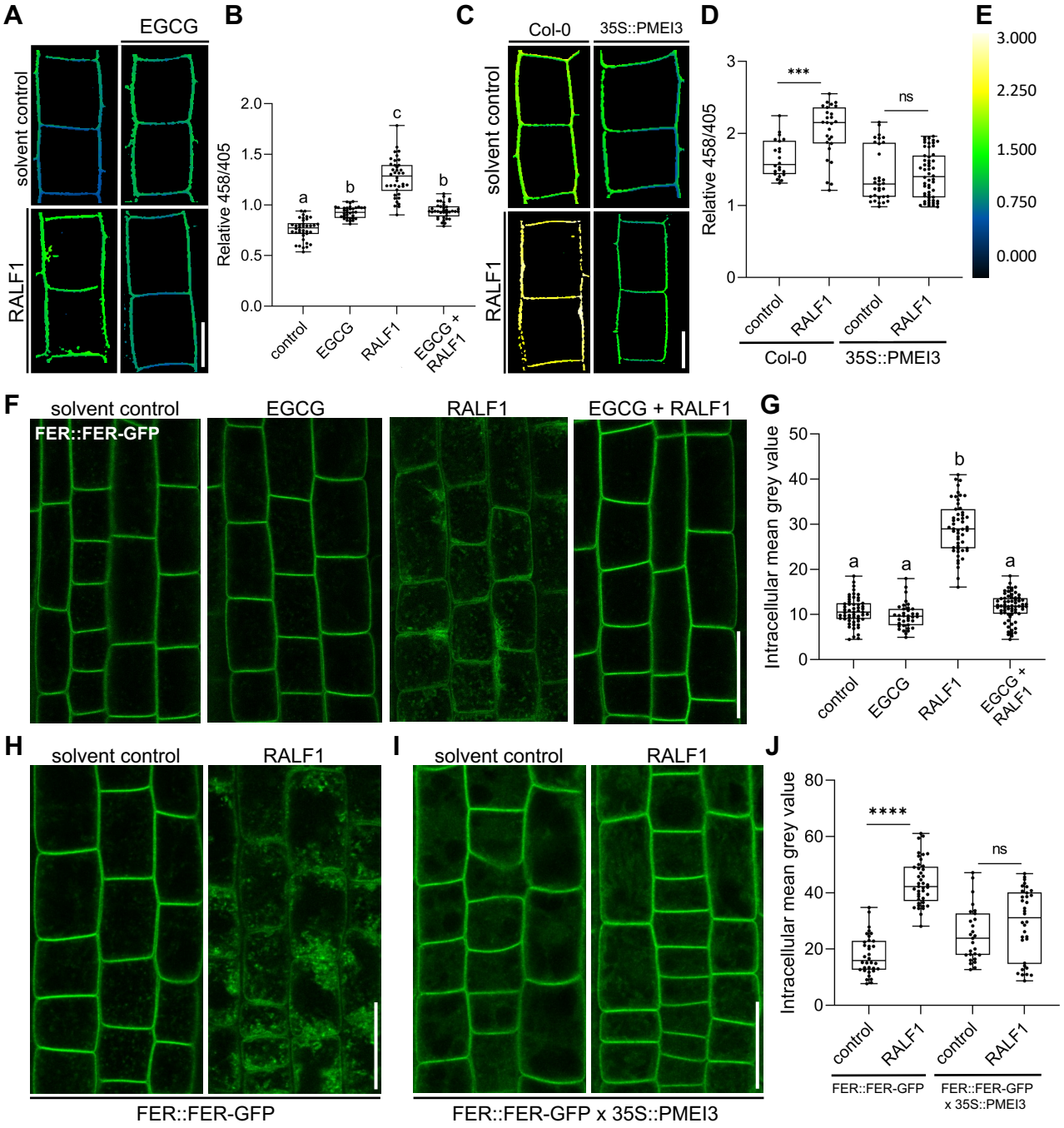
A
EGCG
solvent control
RALF1
B
Relative 458/405
2.0
1.5
1.0
0.5
0.0
a
b
c
b
control
EGCG
RALF1
EGCG + RALF1
C
Col-0
35S::PMEI3
solvent control
RALF1
D
Relative 458/405
3
2
1
0
***
ns
control
RALF1
control
RALF1
Col-0
35S::PMEI3
E
3.000
2.250
1.500
0.750
0.000
F
solvent control
EGCG
RALF1
EGCG + RALF1
FER::FER-GFP
G
Intracellular mean grey value
50
40
30
20
10
0
a
a
b
a
control
EGCG
RALF1
EGCG + RALF1
H
solvent control
RALF1
FER::FER-GFP
I
solvent control
RALF1
FER::FER-GFP x 35S::PMEI3
J
Intracellular mean grey value
80
60
40
20
0
****
ns
control
RALF1
control
RALF1
FER::FER-GFP
FER::FER-GFP x 35S::PMEI3

Figure 4.

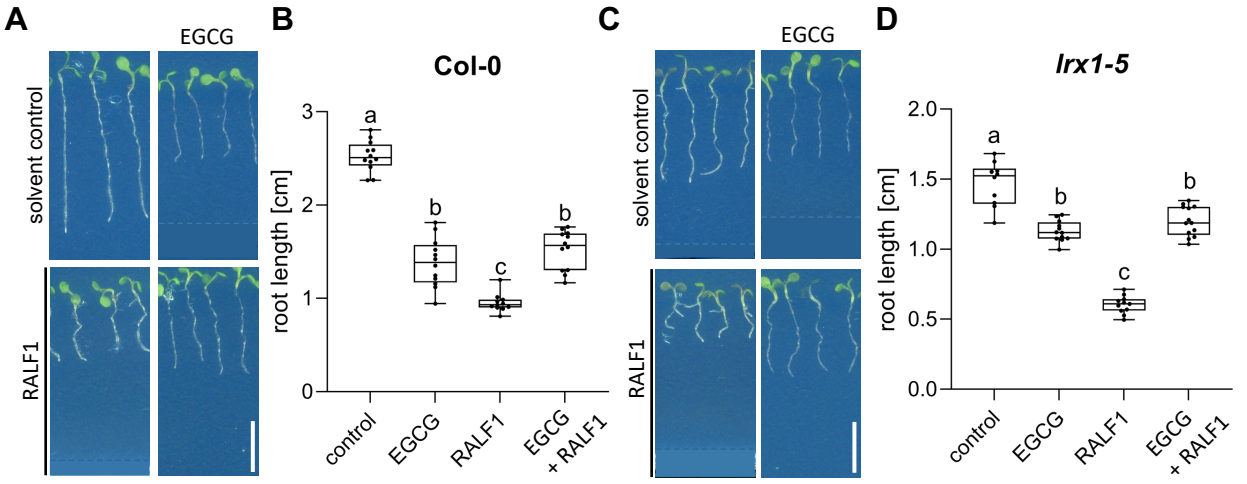
A
EGCG
solvent control
RALF1
B
Col-0
root length [cm]
3
2
1
0
a
b
c
b
control
EGCG
RALF1
EGCG
+ RALF1
C
EGCG
solvent control
RALF1
D
lrx1-5
root length [cm]
2.0
1.5
1.0
0.5
0.0
a
b
c
b
control
EGCG
RALF1
EGCG
+ RALF1

Figure 5.

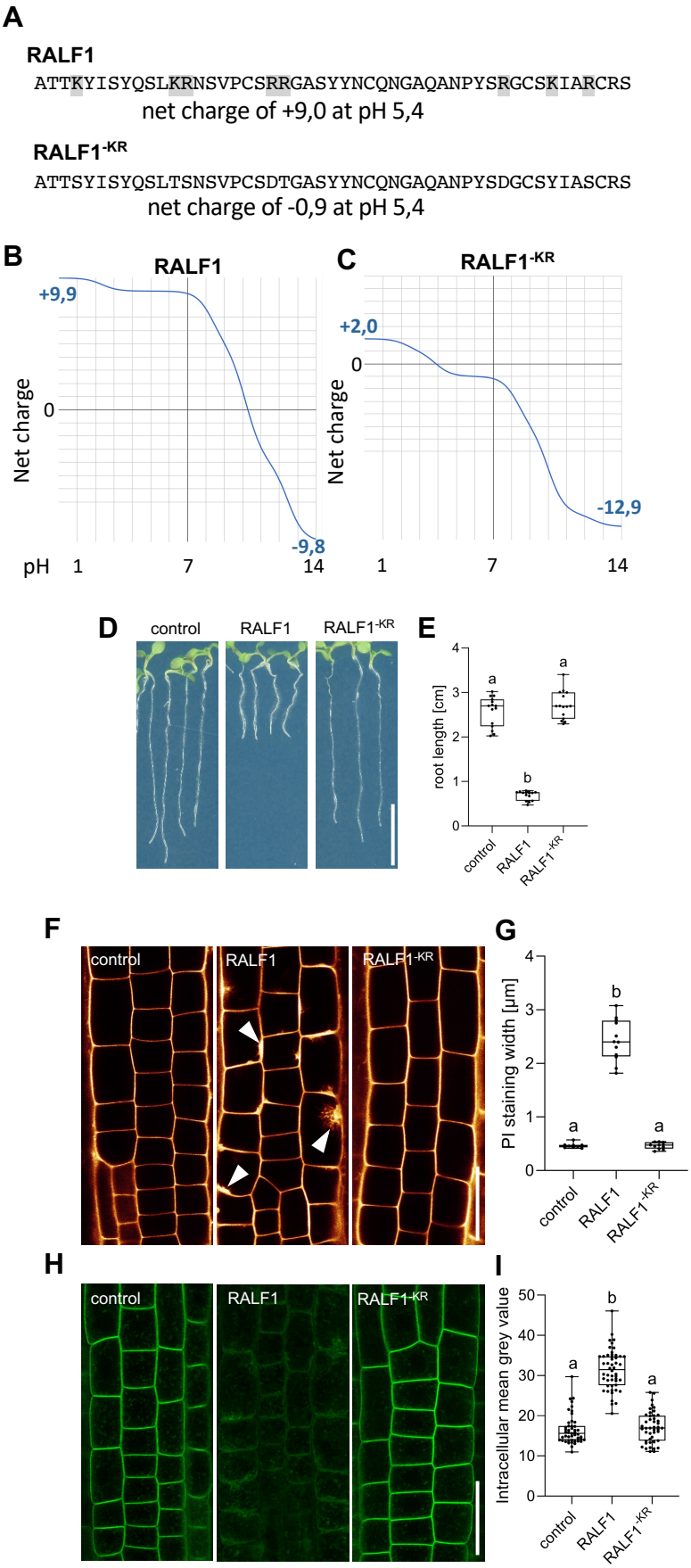
A
RALF1
ATTKYISYQSLKRNSVPCSRRGASYYNCQNGAQANPYSRGCSKIARCRS
net charge of +9,0 at pH 5,4
RALF1-KR
ATTSYISYQSLTSNSVPCSDTGASYYNCQNGAQANPYSDGCSYIASCRS
net charge of -0,9 at pH 5,4
B
RALF1
+9,9
0
-9,8
Net charge
pH 1 7 14
C
RALF1-KR
+2,0
0
-12,9
Net charge
1 7 14
D
control
RALF1
RALF1-KR
E
root length [cm]
a
b
a
control
RALF1
RALF1-KR
F
control
RALF1
RALF1-KR
G
PI staining width [µm]
a
b
a
control
RALF1
RALF1-KR
H
control
RALF1
RALF1-KR
I
Intracellular mean grey value
a
b
a
control
RALF1
RALF1-KR

Figure 6.

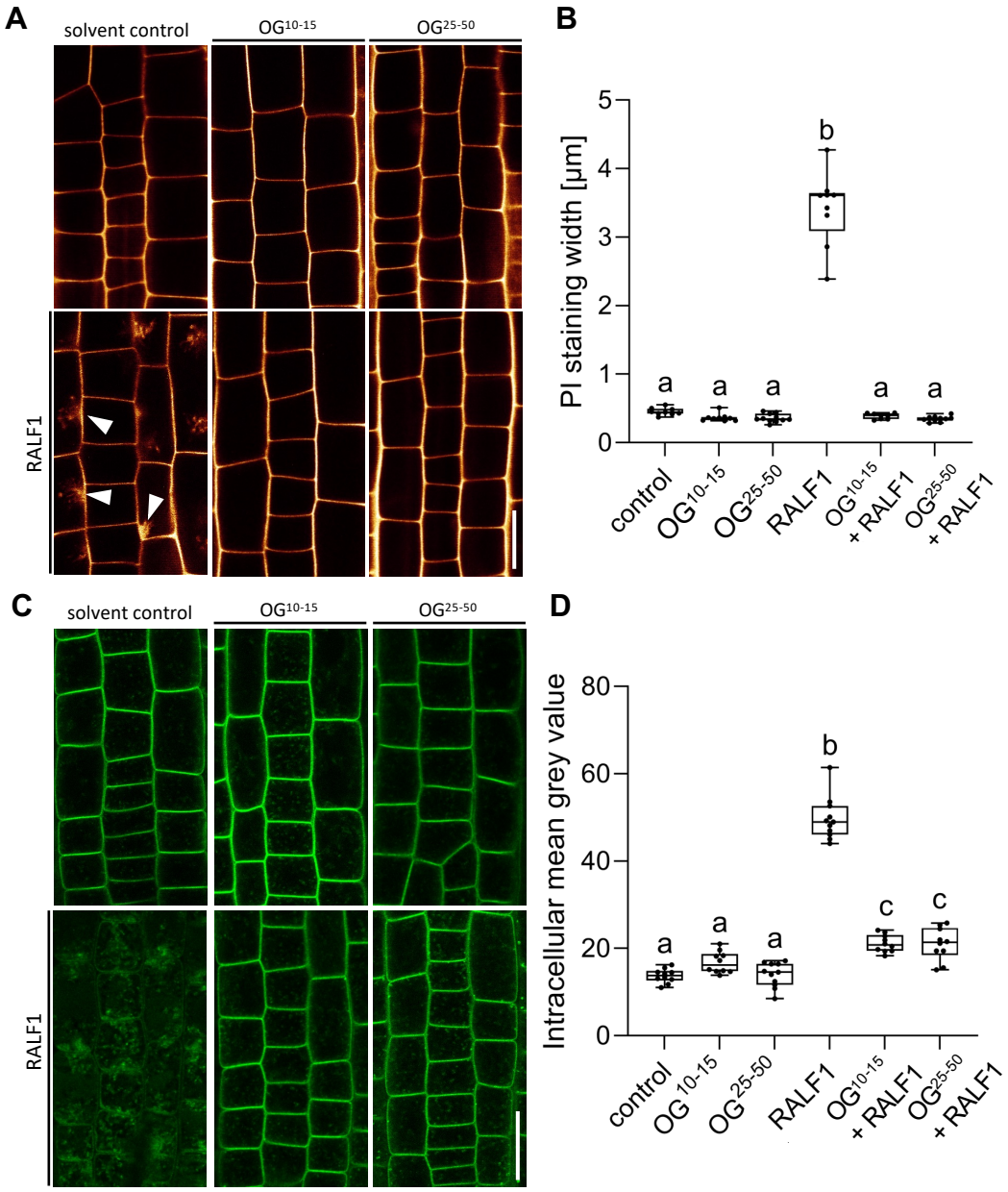
A
solvent control
OG10-15
OG25-50
RALF1
B
PI staining width [µm]
5
4
3
2
1
0
a
a
a
b
a
a
control
OG10-15
OG25-50
RALF1
OG10-15 + RALF1
OG25-50 + RALF1
C
solvent control
OG10-15
OG25-50
RALF1
D
Intracellular mean grey value
80
60
40
20
0
a
a
a
b
c
c
control
OG 10-15
OG 25-50
RALF1
OG10-15 + RALF1
OG25-50 + RALF1

Figure 7.

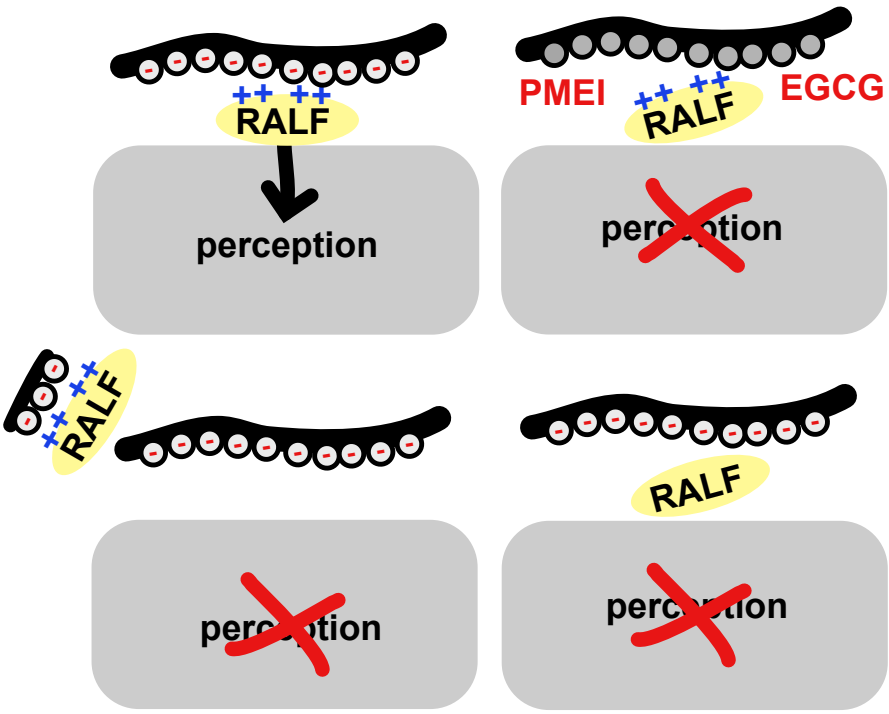
RALF
perception
PMEI
EGCG
RALF
perception
RALF
perception
RALF
perception